Hydrol. Earth Syst. Sci. Discuss., doi:10.5194/hess-2017-152, 2017
Manuscript under review for journal Hydrol. Earth Syst. Sci.
Discussion started: 22 March 2017

Hydrology and Earth System Sciences
Discussions

Use of GNSS SNR data to retrieve soil moisture and vegetation variables over a wheat crop

Sibo Zhang[1,2], Nicolas Roussel[3], Karen Boniface[2,3,4,6], Minh Cuong Ha[3], Frédéric Frappart[5], José Darrozes[3], Frédéric Baup[4], and Jean-Christophe Calvet[1]

[1]CNRM – UMR3589 (Météo-France, CNRS), Toulouse, France

[2]Fondation STAE, Toulouse, France

[3]GET (UMR5563 CNRS/Université Paul Sabatier, UR254 IRD), Toulouse, France

[4]CESBIO, Université de Toulouse, CNES/CNRS/IRD/UPS, Toulouse, France

[5]LEGOS – UMR566 (CNES, CNRS, IRD, UPS), Toulouse, France

[6]now at Joint Research Centre / European Commission, Ispra, Italy

Correspondence to: Jean-Christophe Calvet (jean-christophe.calvet@meteo.fr)

Abstract. This work aims to estimate soil moisture and vegetation characteristics from Global Navigation Satellite System (GNSS) Signal to Noise Ratio (SNR) data using direct and reflected signals by the land surface surrounding a ground-based antenna. Observations are collected over a rainfed wheat field in southwestern France. The retrievals are compared with two independent reference datasets: *in situ* observations of soil moisture and vegetation height, and numerical simulations from the ISBA (Interactions between Soil, Biosphere and Atmosphere) land surface model. Results show that changes in soil moisture mainly affect the multipath phase of the SNR data (assuming the relative antenna height is constant) with little change in the dominant period of the SNR data. Changes in vegetation height are more likely to modulate the SNR dominant period derived from a wavelet analysis. Surface volumetric soil moisture can be estimated ($R^2 = 0.73$, RMSE = 0.014 m^3m^{-3}) when the wheat is smaller than 20 cm. The quality of the estimates markedly decreases when the vegetation height increases. This is because the GNSS signal is less affected by the soil contribution. A wavelet analysis provides an accurate estimation of the wheat crop height ($R^2 = 0.98$, RMSE = 6.2 cm). The latter correlates with modeled above-ground biomass of the wheat from stem elongation to ripening. It is found that the vegetation retrievals are sensitive to changes in plant height of at least one wavelength. A simple smoothing of the retrieved plant height allows an excellent matching to *in situ* observations, and to modeled above-ground biomass.

1 Introduction

In situ observations of soil moisture and vegetation variables are key to validate land surface models and satellite-derived products. Recent international initiatives, such as the International Soil Moisture Network (Dorigo et al., 2013) or the Committee on Earth Observation Satellites (CEOS) Land Product Validation group (Morisette et al., 2006) have improved

the access to such observations. However, they remain very sparse and there is a need to develop new automatic techniques to monitor land surface variables at a local scale. A number of studies demonstrated that Global Navigation Satellite System (GNSS) multipath signals can be used to retrieve various geophysical parameters of the surface surrounding a GNSS receiving antenna (Motte et al., 2016). Over land, variables such as soil moisture, snow depth and vegetation status can be observed (Larson et al., 2008; Small et al., 2010; Larson and Nievinski, 2013; Wan et al., 2015; Boniface et al., 2015; Larson, 2016; Roussel et al., 2016). GNSS satellites operate at the L-band microwave frequency domain (between 1.2 GHz and 1.5 GHz). At these relatively low frequencies, the microwave signal is less perturbed by atmospheric effects and can better penetrate clouds and heavy rains than higher frequency signals. This ensures continuous operations, in all weather conditions, at either daytime or nighttime. The L-band signal emitted or reflected by terrestrial surfaces is related to surface parameters like surface soil moisture, roughness or vegetation characteristics. These properties have been exploited by the Soil Moisture and Ocean Salinity (SMOS) satellite mission for Earth surface remote sensing applications (Kerr et al., 2001). While SMOS is a radiometer and measures the Earth surface microwave emission (passive microwaves), GNSS satellites emit a radar signal (active microwaves). Active microwaves can present improved temporal and spatial resolutions, but the signal may be more sensitive to the structure of the surface, such as soil roughness or vegetation effects than for passive microwaves (Wigneron et al. 1999; Njoku et al. 2002).

Existing geodetic-quality GNSS networks have the potential to provide a large number of *in situ* observations, depending on the receiver technology: (1) waveform acquisition with a specific receiver using two antennas (Zavarotny et al., 2014) or (2) Signal-to-Noise Ratio (SNR) acquisition with classical geodetic receiver (GNSS-IR) using one antenna. GNSS networks can be used to monitor small or large areas depending on the antenna height and satellite elevation (Roussel et al., 2014). Continuous monitoring of surface soil moisture can be made over a long period at spatial scales ranging from 100 m^2 (antenna height of about 2 m) to 8000 m^2 (antenna height of about 150 m) for classical geodetic receiver but can reach a few thousand square kilometers with waveform receivers embedded on satellites (e.g. TechDemoSat-1 mission, Foti et al., 2015). For now, a network called PBO H_2O with GNSS-IR antennas on ground is currently used in western regions of the USA to monitor surface soil moisture (Larson et al., 2013; Chew et al., 2015a) and snow depth (Larson and Nievinski, 2013; Boniface et al., 2015). It must be noted that most of the 161 GNSS antennas of this network are located in mountainous areas or in areas in California characterized by a relatively arid climate. They are surrounded by sparse vegetation.

In GNSS-IR antennas, the interference between the direct and the reflected signals is observed in temporal variations of the SNR data (Bilich and Larson 2007; Zavorotny et al. 2010; Chew et al. 2014). Changes in geophysical or biophysical parameters affect the phase, amplitude and frequency of the SNR modulation pattern. The SNR is also influenced by surface roughness and by the position of the antenna with respect to the surface and to the satellite (Larson and Nievinski 2013; Chew et al. 2015a). The SNR modulation primarily depends on:

- the relative height of the GNSS antenna above the reflecting surface (ground or vegetation surface),
- satellite elevation,

- the superposition of the direct signal and of the reflected signal, which varies along with changes in the satellite track positions,
- Right Hand Circular Polarization (RHCP) and Left Hand Circular Polarization (LHCP) gain pattern of the receiving antenna, (RHCP usually increases the SNR when the satellite elevation angle increases, LHCP is related to imperfections of the antenna and is greater than RHCP for the reflected signal);
- reflection coefficients for the reflecting surface, related to the water content and the ground mineralogical content of the reflecting surface,
- surface topography and roughness and
- the satellite transmitted power.

A soil moisture retrieval algorithm from SNR data was derived by Chew et al. (2014) over bare soil. In a subsequent modeling study Chew et al. (2015a, b) showed that the vegetation canopies affected the SNR modulation pattern. They showed that vegetation growth tended to trigger a decrease of the SNR amplitude. Because the vegetation effects tended to perturb the soil moisture retrieval, Chew et al. (2015a) proposed an improved algorithm for soil moisture retrieval in vegetated environments, which used the amplitude decrease extent to decide when vegetation influence was too large. They used a model database for the SNR of L2C signal to remove most significant vegetation effects for the sites they considered in Western USA. Small et al. (2016) further compared different algorithms of GNSS-IR soil moisture retrieval in the presence of vegetation. Roussel et al. (2016) integrated both GPS and GLONASS SNR data to retrieve soil moisture over bare soil. Using data from a field study, Wan et al. (2014) showed that the amplitude of the SNR data presented a good linear relationship with the vegetation water content (VWC), but it was restricted to VWC values of less than ~1 kg m^{-2}. In addition to the amplitude of the SNR data, it was also possible to infer VWC by the $MP1_{rms}$ index, which is a linear combination of L1 and L2 carrier phase data and L1 pseudorange data (Small et al. 2010), and by the NMRI (Normalized Microwave Reflection Index) which is a normalization result based on the $MP1_{rms}$ (Small et al. 2014; Larson and Small 2014).

In this study, GNSS SNR data were obtained using the GNSS-IR technique, with a single classical geodetic antenna receiver over an intensively cultivated wheat field in southwestern France. The data were used to retrieve soil moisture and vegetation characteristics during the growing period of wheat. The method proposed by Chew et al. (2015a) (hereafter referred to as CH15) was used to retrieve soil moisture. A wavelet analysis was performed in order to extract the dominant period of the SNR and further to retrieve vegetation height. We investigated to what extent vegetation height influenced the dominant period resulting from the wavelet analysis. The main justification for investigating the impact of vegetation height was that it impacted the relative antenna height (the distance from the antenna to the reflecting surface). Vegetation growth tended to decrease the relative antenna height and broke up the constant height assumption used in soil moisture retrieval algorithms. In this context, key objectives of this study were to (1) assess the soil moisture retrieval technique in both sparse and dense vegetation conditions, and (2) retrieve vegetation height along the wheat growth cycle.

Hydrol. Earth Syst. Sci. Discuss., doi:10.5194/hess-2017-152, 2017
Manuscript under review for journal Hydrol. Earth Syst. Sci.
Discussion started: 22 March 2017

2 Data

2.1. SNR data and pre-processing

GNSS SNR data were acquired from an antenna at 2.51 m above the soil surface over an experimental field covered by rainfed winter wheat in Lamasquère, France (43°29'10"N, 1°13'57"E, see Fig. S1 in the Supplement). These GNSS data were collected by GET (Géosciences Environnement Toulouse) for a whole growing season, from January to July 2015. A Leica GR25 receiver equipped with an AS10 antenna was used and data were acquired at a sample frequency rate of 1 Hz. Only the S1C SNR signal strength on the civilian L1 C/A channel of the GPS constellation was used in this study. A number of studies (e.g. Vel et al., 2015) showed that the SNR of the L1 C/A signal can be used to provide reliable soil moisture estimates over sparse vegetation and bare soil surface, although it is less precise than the L2C signal. The quality of the more recently available L2C signal (used by PBO H_2O (CH15)) is higher than either L1 C/A or L2P from non-code tracking receivers. However, the used receiver could not track L2C signals. Although data from other constellations were also acquired (e.g., GLONASS, GALILEO), their orbital parameters such as satellite track positions or satellite altitude were not the same. In order to be consistent with the GPS-only studies of Larson et al. (2008), CH15, and Small et al. (2016), we only used GPS SNR data. For our site, four GPS satellites were excluded from the analysis because their data were incomplete (GPS03, 20, 26, these numbers corresponding to their Pseudo-Random Noise (PRN) numbers) or not received (GPS08). Finally, GPS SNR data were missing for only nine days: 8 and 9 February, 3 April and from 13 to 18 May 2015.

Following the method proposed by Larson et al. (2010), a low-order polynomial was fit to the SNR data, and the modulation pattern was then derived from the SNR by subtracting this polynomial from the SNR data. The logarithmic dB-Hz units were converted to a linear scale in V V^{-1} using the following conversion equation: $SNR_{linear} = 10^{\frac{SNR}{20}}$ (Vey et al., 2015). We only analyzed the modulation patterns in a valid segment for satellite configurations corresponding to low elevation angles, ranging from 5 to 20 degrees. This corresponded to a valid segment data recording of less than one hour (40 to 50 minutes). Avoiding very low elevation angles (less than 5 degrees) limited spurious effects from trees and artificial surfaces surrounding the field. Avoiding high elevation angles (more than 20 degrees) limited the reduction of the multipath signal amplitude. Because the SNR signal amplitude was much reduced and the wave pattern was not visible at high elevations for our field observations, we excluded elevation angles larger than 20 degrees. Figure 1a shows an example of the valid segment of the multipath SNR data for the ascending track of GPS01 on 21 January 2015. The periodic signature of the multipath SNR data is visible.

2.2. Soil moisture and vegetation characteristics

The GNSS data were acquired over a rainfed wheat field in 2015. This field campaign was a part of a coordinated effort by CESBIO (Centre d'Etudes Spatiales de la BIOsphère) to monitor crops in southwestern France using both *in situ* and satellite observations. Independent *in situ* observations of soil moisture and vegetation variables were made together with model

simulations of these quantities. Both observations and simulations were used to validate soil moisture and vegetation height retrievals. Since the whole wheat growing cycle was considered, both soil moisture and vegetation modulated the multipath SNR pattern. Soil roughness was considered as stable in time from sowing to harvest.

The wheat was sown during the autumn, on 1 October 2014 and was harvested from 26 to 30 June 2015. Volumetric soil moisture (VSM) was continuously monitored at a depth of 5 cm from 16 January to 10 March 2015 and from 30 March to 26 May 2015. Measurements of crop height were performed at seven dates during the plant growing cycle. The canopy height did not exceed 0.1 m at wintertime and rapidly increased at springtime: it reached 0.2 m on 10 March 2015 and about 1 m at the end of May.

In addition to *in situ* observations, simulations of surface soil moisture (0-10 cm top soil layer), plant height and above-ground biomass were performed for this site by CNRM (Centre National de Recherches Météorologiques) using the ISBA (Interactions between Soil, Biosphere, and Atmosphere) land surface model within the SURFEX (version 7.2) modeling platform (Masson et al. 2012). The ISBA configuration and the atmospheric analysis we used to force the model are described in Lafont et al. (2012). The C3 crop plant functioning type and a multilayer representation of the soil hydrology were considered. These simulations were used as an independent benchmark for soil moisture and vegetation variables.

3. Methods

As noted by Georgiadou and Kleusberg (1988) and Bilich and Larson (2007), assuming the ground surface is horizontal, the additional distance (δ) travelled by a reflected signal relative to the direct signal is

$$\delta = 2h\sin(\theta) \tag{1}$$

where h is the relative antenna height, and θ is the satellite elevation angle. This path delay δ can also be expressed in terms of the multipath relative phase ψ :

$$\psi = 2\pi\frac{\delta}{\lambda} \tag{2}$$

where λ represents the L1 wavelength (0.1903 m).

Thus the multipath frequency (f) and period (T) can be written as:

$$\omega = 2\pi f = \frac{d\psi}{dt} = \frac{4\pi}{\lambda}h\cos(\theta)\frac{d\theta}{dt} \tag{3}$$

$$\frac{1}{T} = f = \frac{2h\cos(\theta)}{\lambda}\frac{d\theta}{dt} \tag{4}$$

This means that the relative antenna height (h) directly affects multipath frequency f and period T. Antennas far above the reflecting surface have higher multipath frequencies (smaller multipath periods) than antennas closer to the reflecting surface. Furthermore, satellite geometric information and motion substantially influences the period (T) of the multipath

Hydrol. Earth Syst. Sci. Discuss., doi:10.5194/hess-2017-152, 2017
Manuscript under review for journal Hydrol. Earth Syst. Sci.
Discussion started: 22 March 2017

SNR data due to the $\cos(\theta)$ and $d\theta/dt$ terms in equation (4). If satellite passes reach high elevation angles (e.g., GPS01 in Supplement Fig. S2), $d\theta/dt$ becomes large. Conversely, satellites signals observed at small maximum elevations (e.g., GPS18 in Supplement Fig. S2) move more slowly (small $d\theta/dt$) than satellites passing overhead (Bilich and Larson 2007). In order to limit the impact of these differences from satellite motion, only the full-track data with at least 40 degree maximum elevation angle were selected. Among the remaining tracks we further removed the slowly moving tracks whose maximum $\cos\theta \cdot d\theta/dt$ was less than 9.5×10^{-5} rad s^{-1} (threshold value based on our field observations) of the valid segment (elevation angles ranging between 5 and 20 degrees). This specific data sorting was only made for vegetation height retrieval. After this selection, the number of available satellite tracks was 37 per day.

3.1. Soil moisture retrieval

For bare soil, changes in surface soil moisture affect the signal penetration depth. The latter can be very small in wet conditions and tends to increase in dry conditions, up to a few centimeters (Chew et al., 2014; Roussel et al., 2016). This is a small change with respect to the antenna height (2.51 m in this study). Consequently, the relative antenna height (h) is considered as a constant (h_c=2.51m) in the following. Using sine of the elevation angle ($\sin(\theta)$) as the independent variable, the modulation frequency becomes proportional to h_c. Then the multipath SNR can be expressed as (Larson et al., 2008):

$$SNR_{mpi} = A\cos(\frac{4\pi h_c}{\lambda}\sin(\theta) + \varphi_{mpi}) \quad (5)$$

The least square estimation (LSE) method proposed by Larson et al. (2008) is used to estimate the multipath amplitude (A) and multipath phase (φ_{mpi}) from the multipath SNR data. Then, φ_{mpi} can be further used to estimate the soil moisture changes because φ_{mpi} is sensitive to very fine frequency changes triggered by small changes in the apparent penetration depth of the wave (Larson et al., 2008; Larson et al., 2010; Chew et al., 2014; CH15; Roussel et al., 2016). Various empirical models were proposed to estimate soil moisture from this quantity (Larson et al. 2008; Chew et al. 2014; Vey et al., 2015), and the best results are obtained using a linear model. We used a linear relationship between φ_{mpi} and soil moisture to retrieve volumetric soil moisture content (VSM in m^{3}m^{-3}) time series for conditions with no significant vegetation effects (CH15),

$$VSM_t = S \cdot \Delta\varphi_t + VSM_{resid} \quad (6)$$

Phase changes $\Delta\varphi_t = \varphi_t - \varphi_0$ are calculated with respect to φ_0, the reference phase. We used the method proposed by CH15 consisting in estimating φ_0 as the mean of the lowest 15% of the φ_{mpi} data for each track during the retrieving period. The same condition is used to estimate the VSM_{resid} residual soil moisture from the *in situ* VSM observations. The

Hydrol. Earth Syst. Sci. Discuss., doi:10.5194/hess-2017-152, 2017
Manuscript under review for journal Hydrol. Earth Syst. Sci.
Discussion started: 22 March 2017

VSM_{resid} was taken as the minimum soil moisture observation, which presented a value of 0.252 m^3m^{-3} during the retrieving period. The S parameter (in $m^3m^{-3}degree^{-1}$) is the slope between phase changes and soil moisture. For time series with no significant vegetation effects, S = 0.0148 $m^3m^{-3}degree^{-1}$ for L2C signal (CH15). We also used the *in situ* volumetric soil moisture observations (VSM_t), $\Delta\varphi_t$ and VSM_{resid} to fit the local adjusted slope in order to check the a priori slope value given by CH15, see Sect. 4.1.

CH15 defined the normalized amplitude (A_{norm}) as the ratio of amplitude to the average of the top 20 % amplitude values. The A_{norm} time series can be used to assess whether or not vegetation effects are significant. Values of A_{norm} above 0.78 (dimensionless) indicate that vegetation effects are small (CH15). In conditions of significant vegetation effects CH15 used an algorithm able to correct the phase for vegetation effects. This algorithm is based on an unpublished lookup table. Since we were not able to correct for vegetation effects we retrieved surface soil moisture during a period with rather sparse vegetation, from 16 January to 5 March. During this time span, A_{norm} was above 0.78 as shown in Fig. 2 (black dots). Following CH15, the median soil moisture estimate from all available satellite tracks that passed at different times during the day was used as the final soil moisture estimate.

3.2. Vegetation height retrieval using a wavelet analysis

While vegetation grows, the vegetation surface gradually replaces the bare soil surface as the dominant reflecting surface. As a consequence, the height (h) of the antenna above the reflecting surface decreases. Equation (4) shows that changes in h impact the multipath frequency f and consequently T. This property allows the use of changes in T values to infer changes in h, and further estimate vegetation height. The wavelet analysis is well suited for analyzing time series with non-stationary power and frequency changes across time as illustrated by Fig. 1. The wavelet analysis methodology and the WaveletComp R-package (Roesch et al., 2014) were used to analyze the period structure and evaluate the power spectrum of the multipath SNR signal (see the Supplement).

Figure 1 shows an example of SNR time series (black line) from the ascending track of GPS01 on 21 January 2015. Its average power spectrum derived from a wavelet analysis is also shown, together with the power spectrum for periods ranging from 128 to 1024 s. From the average power spectrum, there is only one peak and the corresponding peak period is 362 s. The SNR data is reconstructed depending on this peak period (red line in Fig. 1a), which is a good fit to the SNR data. Both phases and amplitudes match well. This shows that the peak period from the average power spectrum can be used to represent the SNR data. Limiting elevation angle values from 5 to 20 degrees (Sect. 2.1) ensures a relatively stable value of the peak period. The peak period is considered as the dominant period (T_d) of the SNR data.

During the wheat growth cycle, preliminary tests showed that the average power spectrum could present multiple peaks together with a reduced maximum average power. This made T_d unsuitable for the representation of the multipath SNR data. Under this situation the quality of the T_d value was considered as poor and the data were not used. We sorted out the data acquired in two situations: (1) track data presenting more than one peak in the highest 80% percentile of the power spectrum, (2) T_d value smaller by 10 seconds than the mean value of the lowest 10% of the dominant periods (e.g., T_d < 352 s for

Hydrol. Earth Syst. Sci. Discuss., doi:10.5194/hess-2017-152, 2017
Manuscript under review for journal Hydrol. Earth Syst. Sci.
Discussion started: 22 March 2017

Hydrology and Earth System Sciences Open Access EGU Discussions

GPS01). This is illustrated in the Supplement (Figs. S3 and S4). The probability distribution (grey bars) of bad quality tracks among all available satellite tracks is shown in Fig. 2 on a daily basis from 16 January to 15 July 2015. Most unsuitable tracks are observed during two time periods: (1) at the beginning of spring, from 10 to 20 March, and (2) at the beginning of summer, from 12 to 26 June. The latter corresponded to lodging of vegetation, which occurred during a strong wind event and affected the reflecting surface height. The *in situ* observation of wheat height was only 39 cm on 18 June.

As shown in Sect. 3.1, vegetation effects on the SNR signal became significant after 5 March. After this date, A_{norm} (black dots in Fig. 2) decreased drastically, in relation to plant growth. After 10 March, wheat height exceeded one wavelength (> 0.19 m). In addition to lower A_{norm} values, an increasing number of unsuitable tracks was observed till 20 March, together with low values of T_d (see Supplement Fig. S4). One possible reason is that during the 10-20 March period, the reflected GNSS signal included contributions from both soil and vegetation. Before this period, the soil contribution was dominant. After 10 March, the vegetation gradually decreased the strength of the signal reflected from the soil surface. When the vegetation surface completely replaced the soil surface as the dominant reflecting surface of the GNSS signal, a single peak period was observed again and its value increased in response to the rise of the reflecting surface. For example, T_d increased from 362 s (10 March) to 397 s (22 March) for GPS01 ascending tracks (Supplement Fig. S4). At the same time, A_{norm} also increased but remained below 0.6 maybe because the water content of vegetation attenuated part of the reflected GNSS signal. Figure S4 shows that T_d is not sensitive to vegetation height when vegetation height is smaller than one wavelength. Therefore, we concluded that this vegetation height retrieval technique was not working for vegetation height below one λ and when multiple peaks were observed in the average power spectrum.

Additionally, the major part of the signal power is concentrated on elevation angles ranging from 7 to 11 degrees (see Fig. 1). A preliminary analysis for the entire wheat growing cycle showed that, more often than not, the elevation angle corresponding to the peak power was around 9 degree. In this study, elevation and its change rate at 9 degree are used to represent the SNR data for all available satellite tracks. It must be noted that this reference elevation angle is specific to the gain pattern and height of the antenna encountered in this experiment. It could present different values in other antenna configurations.

After obtaining the dominant period (T_d) time series, the relative antenna height (h) can be derived from Eq. (4) as:

$$h = \frac{\lambda}{2\cos\theta_{E9} \cdot \frac{d\theta_{E9}}{dt} \cdot T_d} \tag{7}$$

The T_d value is used to represent the multipath SNR data in order to estimate h. Also, changes in the elevation angle (θ) and in $d\theta/dt$ have to be accounted for. This means that h is a variable depending on the elevation angle. In this study, changes in h were surveyed across dates at an elevation angle of 9 degree.

Changes in relative antenna height (h) are directly related to vegetation height increase:

$$\Delta H = h_0 - h \tag{8}$$

Hydrol. Earth Syst. Sci. Discuss., doi:10.5194/hess-2017-152, 2017
Manuscript under review for journal Hydrol. Earth Syst. Sci.
Discussion started: 22 March 2017

Hydrology and Earth System Sciences
Open Access
Discussions

Similarly to the phase change estimates ($\Delta\varphi_t$ in Sect. 3.1), h_0 is the median value of the top 15% h data during the whole wheat growth cycle for each track.

The final retrieved vegetation height (H) is based on the mean height change from all available satellite tracks (N = 37), plus one wavelength:

$$H = \frac{\sum_{N} \Delta H}{N} + \lambda \tag{9}$$

The minimum value of H is one wavelength. Therefore Eq. (9) can only be applied when the wheat height is higher than one wavelength (0.19 m).

3.3. Scores

The mean absolute error (MAE) is a quantity used to measure how close retrievals are to the observations, MAE is given by

$$MAE = \frac{1}{n}\sum_{i=1}^{n}\left|VSM_i^{OBS} - VSM_i^{GPS}\right| \tag{10}$$

VSM^{OBS} represents the *in situ* VSM observations, VSM^{GPS} represents the retrieved soil moisture by GPS data, n is the valid number of data.

The root mean square error (RMSE) represents the sample standard deviation of the differences between retrieved values and observed values:

$$RMSE = \sqrt{\frac{\sum_{i=1}^{n}\left(VSM_i^{OBS} - VSM_i^{GPS}\right)^2}{n}} \tag{11}$$

The standard deviation of the difference between observations and retrievals (SDD) is

$$SDD = \sqrt{\frac{\sum_{i=1}^{n}(x_i - \bar{x})^2}{n}} \tag{12}$$

$x_i = VSM_i^{GPS} - VSM_i^{OBS}$, $\bar{x}$ is the mean value of x.

The fraction of explained variance is represented by the squared Pearson correlation coefficient, R^2.

Hydrol. Earth Syst. Sci. Discuss., doi:10.5194/hess-2017-152, 2017
Manuscript under review for journal Hydrol. Earth Syst. Sci.
Discussion started: 22 March 2017

4. Results

4.1 Soil moisture retrieval

Figure 3 presents the surface soil moisture retrievals from 16 January to 5 March 2015, together with independent *in situ* VSM observations and ISBA simulations. The VSM retrievals are derived from GPS SNR observations using Eq. (6) in sparse vegetation conditions, when A_{norm} is above 0.78 (see Sect. 3.1). The method proposed by CH15 is used, with S = 0.0148 $m^3m^{-3}degree^{-1}$. We also used the *in situ* soil moisture observations (Sect. 3.1) and phases from SNR data to fit the local slope: S = 0.0033 $m^3m^{-3}degree^{-1}$. This adjusted slope value is the mean of slope values obtained for satellite tracks whose phase presents a linear correlation with *in situ* soil moisture higher than 0.9. This occurred for the ascending tracks of GPS 13, 21, 24, 30 and for the descending tracks of GPS 05, 09, 10, 15, and 23. The VSM retrievals obtained using S = 0.0033 $m^3m^{-3}deg^{-1}$ are shown in Fig. 4. The GPS and ISBA scores are given in Table 1.

In both Figs. 3 and 4, the sub-daily statistical distribution of the VSM retrievals is indicated by box plots. The range of daily standard deviation value of the various VSM estimates is shown in Table 2. The *in situ* VSM measurements present the smallest sub-daily variability, with a mean standard deviation value of 0.002 m^3m^{-3}. The largest variability is obtained for the GPS retrievals based on the priori slope value S = 0.0148 $m^3m^{-3}deg^{-1}$, with a mean standard deviation value of 0.036 m^3m^{-3}. GPS retrievals based on the adjusted slope value S = 0.0033 $m^3m^{-3}deg^{-1}$ presents intermediate values (0.008 m^3m^{-3}), together with the ISBA simulations (0.005 m^3m^{-3}). Figures 3 and 4 show that the sub-daily variability of GPS VSM retrievals tends to increase during the last 10 days of the retrieval period.

It must be noted that GPS data are missing on 8 and 9 February, and that the ISBA simulations indicate soil freezing (i.e. the presence of ice in the top soil layer) from 4 to 9 February. This period was excluded from the comparison. In the end, there were 47 valid observation days for the statistical analysis of the retrieved surface VSM, among which 43 days could be compared with model simulations.

The GPS VSM daily mean retrievals based on the CH15 method present a good agreement with both *in situ* observations and ISBA simulations: MAE and RMSE are lower than 0.05 m^3m^{-3}, and SDD does not exceed 0.04 m^3m^{-3} (Table 1). The errors are reduced by at least 50 % when the local adjusted slope is used.

Figure 5 shows the retrieved soil moisture as a function of the *in situ* observations for a priori and adjusted slopes (S = 0.0148 $m^3m^{-3}deg^{-1}$ and S = 0.0033 $m^3m^{-3}deg^{-1}$, respectively) from all available satellite tracks, not only those tracks used for fitting the slope (see Supplement Fig. S5). The corresponding improvements in score values are given in Table 1: the MAE decreases from 0.036 to 0.011 m^3m^{-3}, the RMSE decreases from 0.046 to 0.014 m^3m^{-3}, the SDD decreases from 0.036 to 0.009 m^3m^{-3}. The retrievals based on the *a priori* slope markedly overestimate VSM in wet conditions. On the other hand, the retrievals based on the adjusted slope only slightly underestimate VSM. This shows that adjusting the slope is critical and has a major impact on the retrieval accuracy.

We also compared the retrievals with the independent ISBA simulations. The ISBA model VSM simulations present a better agreement with the *in situ* VSM observations than the GPS retrievals, for all the scores, as shown by Table 1 (last column)

and Fig. 4. In particular, R^2 = 0.88 for ISBA simulations, against R^2 = 0.73 for GPS retrievals. This shows that the ISBA simulations can be used as a reference to assess local GPS retrievals. The statistical scores resulting from the comparison between the GPS retrievals and the simulations are similar to those based on *in situ* observations.

After 5 March, A_{norm} drops below 0.78 (Fig. 2), and the VSM retrievals are not valid. We made an attempt to retrieve VSM from 6 to 16 March. We obtained 10 VSM retrieved values and we compared them with ISBA VSM simulations, because *in situ* observations were lacking. The retrievals looked more sparse (not shown) and the R^2 score decreased from 0.63 (Table 1) to only 0.21. This result confirms that the A_{norm} threshold is a good way to assess the VSM retrieval feasibility over vegetated areas.

4.2 Vegetation height retrieval

Figure 6 shows the retrieved vegetation height from 16 January to 15 July 2015, together with seven *in situ* vegetation height measurements and daily vegetation height simulations by ISBA. Since the original H retrievals present a marked levelling effect, the moving average of the GPS height retrievals computed using a centred gliding window of 21 days is shown. The differences between the seven *in situ* observations and the original H retrievals were -8.4 cm, +4.3 cm, -5.4 cm, -10.3 cm, -5.9 cm, -1.7 cm, -1.5 cm. Most of them exhibited a negative bias. Comparing with the errors between the *in situ* observations and the ISBA simulations (-5.4 cm, +5.5 cm, +10.4 cm, -15 cm, -3 cm, 0 cm and -61 cm), the GPS retrievals were closer to the observations on 30 March and 24 April (the third and forth *in situ* observations). On 18 June, the last height *in situ* observation before harvest was 39 cm in relation to lodging. The GPS retrieval was very close to this value with only -1.5 cm error. On the other hand, the ISBA simulation on 18 June was still at 1 m with an error of -61 cm, because the wheat height was simulated without accounting for lodging. This result shows that the *in situ* GPS height retrievals are able to detect local changes in vegetation height. Figure 6 and the scores given in Table 3 show that the GPS retrievals are closer to the observed growing trend than the ISBA simulations. Additionally, the moving average height presents a much better fit to the *in situ* measurements than the raw GPS retrievals. We also compared the GPS retrievals with the ISBA model simulations. We obtained the following score values from 10 March to 11 June 2015: MAE = 8.9 cm, RMSE = 12.4 cm and R^2 = 0.89. Similar values were obtained for the comparison between the moving average height and ISBA simulations: MAE = 9.0 cm, RMSE = 11.6 cm and R^2 = 0.91.

Figure 6 also shows that the retrieved vegetation height is related to the simulated above-ground dry mass of the wheat (brown line) from 10 March to 11 June 2015. The correlation coefficient between the GPS retrieved height and the simulated dry mass (with 87 valid data) is 0.98, and the correlation coefficient between the moving average height from GPS retrievals and the simulated dry mass is 0.99.

Hydrol. Earth Syst. Sci. Discuss., doi:10.5194/hess-2017-152, 2017
Manuscript under review for journal Hydrol. Earth Syst. Sci.
Discussion started: 22 March 2017

5. Discussion

5.1. Can soil moisture be retrieved under significant vegetation effects?

We tested the relationship between the multipath phase in Eq. (5) and soil moisture for the whole wheat growing cycle (see Supplement Fig. S6). We found that when the vegetation effects are not significant (A_{norm} > 0.78), the multipath phase correlates well (R = 0.92) with the *in situ* soil moisture observations. But when the vegetation effects are significant (A_{norm} < 0.78), the unwrapped multipath phase is no longer related to soil moisture. This is consistent with CH15, who showed that soil moisture cannot be retrieved unless vegetation effects are corrected for.

Additionally, we also tested the validity of the empirical threshold (0.78) of A_{norm}. In Fig. S7, it seems that increasing the A_{norm} threshold from 0.78 to 0.88 is better to decide whether or not vegetation effects are significant for our 6-month field data. Using this new threshold, four more days (2-5 March) are excluded. From Figs. 3 and 4, the maximum retrieval differences for these days are around 0.03 m^3m^{-3}, and the 25-75% percentile interval is larger. This shows the A_{norm} threshold (0.78) can be used over rainfed winter wheat field provided errors of 0.03 m^3m^{-3} are considered as acceptable.

5.2. Why does the locally adjusted S parameter differ from CH15 ?

Since the lookup table from CH15 for correcting dense vegetation effects is not available and was built based on the L2C signal, we retrieved soil moisture only when the vegetation effect was small (i.e. when A_{norm} > 0.78). In our experiment, the possible VSM retrieval duration was less than two months, in relatively wet conditions and VSM varied little: 0.25 m^3m^{-3} < VSM < 0.30 m^3m^{-3}. This is probably not enough to represent the full yearly range of soil moisture. This might affect the representativeness of the S parameter (Sect. 3.1) we derived from our field observations. Furthermore, the different signal wavelength (L1 = 19.03 cm, L2 = 24.45 cm) and the different antenna gain pattern might also affect the fitted slope. All these factors contribute to changes in S.

The soil moisture retrieval accuracy, in terms of MAE, RMSE or SDD, depends to a large extent on the adjustment of the slope. However, the Pearson correlation coefficient is not affected by the slope value (same R^2 scores in Table 1). This shows that a scaled soil wetness index can be derived from the GPS retrievals in sparse vegetation conditions without a priori knowledge of the slope. Additionally, it could be useful to integrate other GNSS constellations. In a field experiment over bare soil, Roussel et al. (2016) showed that the R score value of VSM can reach 0.9 with both GPS and GLONASS data.

5.3. Can vegetation characteristics be inferred from the wavelet analysis?

Figure 6 shows that the retrieved vegetation height is consistent with independent estimates. However, vegetation height is not the only factor affecting the reflected GPS signal. Vegetation water content (VWC, in kg m^{-2}) may also play a role on the reflected GPS signal. *In situ* observations indicate that VWC increased together with H during the growing period, from March to mid-May. From mid-May to harvest, VWC tended to decrease but H also decreased in relation to lodging. Can this

specific behavior of VWC be detected from the results of the wavelet analysis? The latter provides three quantities: the dominant period (Sect. 4.2), A_{norm}, and the peak power.

The amplitude (A_{norm}) is related to some extent to VWC (see Sect. 3.2). However, A_{norm} is calculated assuming the relative antenna height is constant. Because the wheat height increased from 10 cm to 100 cm, the relative antenna height was reduced, and this assumption was not satisfied. This affected the estimates of the amplitude of the multipath SNR data, especially when the wheat was tall (see the Supplement Fig. S8). Therefore, it is difficult to unequivocally relate A_{norm} to vegetation characteristics, as illustrated in Fig. 2. However, the drop in A_{norm} observed at the beginning of June (Fig. 2) could be related to the drop in VWC.

From the wavelet analysis, we also obtained the peak power when we searched for the peak period from the average power spectrum. Peak power can represent changes in the multipath SNR strength. Figure 7 shows daily box plots of the peak power for all available satellite tracks from 16 January to 15 July 2015, together with the distribution of bad quality tracks (as in Fig. 2), and rainfall. There are two major possible causes for a sudden reduction of the strength of the reflected SNR signal: (1) the attenuation of the signal by the rain intercepted by vegetation or in the troposphere and (2) the occurrence of more than one dominant reflecting surface at different heights, and this two causes can occur at the same time.

Three events of rapid reduction of the peak power can be observed in Fig. 7. These events are related to larger standard deviation values of vegetation height retrievals (see Fig. S9). The last event in June could be related to lodging. It seems that these events are not related to rainfall events, and that the attenuation by intercepted water content is not a major cause of peak power drops. On the other hand, the emergence of multiple peaks and of bad quality tracks is consistent with the rapid power reduction in March and June. Multiple peaks may indicate that the reflected signal originates from surfaces at different heights. A possible cause of multiple peaks is a more heterogeneous wheat canopy density during the first stage of the growing period and after lodging. In such sparse or mixed vegetation conditions, VWC is not uniformly distributed and the soil surface may significantly contribute to the SNR. In the middle of April, there is no such effect but STD increases (Fig. S9). It is interesting to note that the peak power drops in Fig. 7 correspond to rapid changes in the retrieved vegetation height at multiples of λ or 0.5λ.

5.4. Can unwrapped multipath phase be used to retrieve vegetation height?

The relationship between the multipath phase (Fig. S10) in Eq. (5) and vegetation height was investigated. Because changes in relative antenna height exceeded λ during vegetation growth, the multipath phase had to be unwrapped. Multipath phase presented little changes when the vegetation height was smaller than λ (before 10 March), and it also tended to be relative stable (around 10 degrees) from 21 March to 18 April. From 19 April to 11 June, the variability increased (Fig. S10), and no relationship with plant growth could be found. This indicates that it is better to use the dominant period to retrieve vegetation height than the multipath phase. Moreover, it shows that both multipath phase and dominant period are relatively stable when the vegetation height is smaller than λ. Both tend to aggregate at several value levels.

Hydrol. Earth Syst. Sci. Discuss., doi:10.5194/hess-2017-152, 2017
Manuscript under review for journal Hydrol. Earth Syst. Sci.
Discussion started: 22 March 2017

5.5. Can wheat phenological stages be inferred?

Figure 7 shows that the occurrence of multiple peaks together with a drop of the peak power can be used as an indicator of the start of the most active part of the growing season, and of the end of the senescence period preceding the harvest. Because of the lack of *in situ* records of the field wheat growth stages, we built a reference growing degree days (GDD) model based on the wheat growth stage dates observed at the same location in 2010 (Fieuzal et al. 2013, Betbeder et al. 2016). We applied the GDD model to year 2015 and we obtained the following dates for tillering, flowering, and ripening: 12 March, 31 May, and 3 June, respectively (see Fig. S11 in the Supplement). The obtained tillering date (12 March) is close to the start date (10 March) of the multiple peaks (see Sections 3.2 and 5.2).

Tillering in wheat triggers nitrogen uptake and the accumulation of biomass (Gastal and Lemaire, 2002). This is consistent with the rapid changes in the indicators derived from the wavelet analysis: drop in A_{norm} values and high rate of multiple peaks (Fig. 2), rise in the retrieved H (Fig. 6), and drop in peak power (Fig. 7). For our site, the tillering date also corresponds to the period when H reached a value of about 0.2 m. This was the case in 2015 (Sect. 3.2) and in 2010 (Betbeder et al. 2016).

Flowering and ripening do not trigger abrupt changes in the GPS retrievals. However, these stages correspond to a change in H trend. This is illustrated in Supplement Fig. S12, which shows the difference of H with the H value retrieved 15 days before. Flowering and ripening occur when this difference gets close to zero, at the end of the growing period.

6. Conclusions

In this study, SNR observations of GPS L1 C/A signal were used to retrieve soil moisture and vegetation height over a rainfed wheat field in southwestern France. A new algorithm based on a wavelet analysis was implemented. The dominant period was derived from the average power spectrum and was used to retrieve vegetation height. The method proposed by CH15 was used to retrieve soil moisture under sparse vegetation conditions, before wheat tillering. Soil moisture was retrieved on a daily basis with a precision (SDD) of 0.009 m^3m^{-3}. During and after tillering, wheat growth gradually raised the reflecting surface of the GPS signal, from the soil surface to the vegetation surface, which significantly modulated the dominant period of the multipath SNR data. In these conditions, vegetation effects could not be ignored and soil moisture could not be retrieved. The retrieved vegetation height was in good agreement with the *in situ* observations, and was consistent with a lodging event. However, the retrieved height consisted of several levels. Using a moving average on the retrieved height permitted a better match with the *in situ* height measurements: a precision of 3.8 cm could be achieved, against 5.5 cm for the original retrievals. Furthermore, several indicators derived from the wavelet analysis could be used to detect tillering.

The retrieved vegetation height was based on the dominant period of the average power spectrum. The latter was derived from GPS multipath SNR data for elevation angles between 5 and 20 degrees. We only considered the dominant period variations, without accounting for instantaneous phase changes. The accuracy of the retrieved vegetation height could

Hydrol. Earth Syst. Sci. Discuss., doi:10.5194/hess-2017-152, 2017
Manuscript under review for journal Hydrol. Earth Syst. Sci.
Discussion started: 22 March 2017

probably be improved considering changes in both period and phase of the multipath SNR oscillations. Furthermore, integrate different wavelength SNR data (e.g., L1, L2 and L5) could also be helpful to survey canopy characteristics.

Acknowledgments. The work of Sibo Zhang and Karen Boniface was supported by the STAE (Sciences et Technologies pour l'Aéronautique et l'Espace) foundation, in the framework of the PRISM (Potentialités de la Réflectométrie GNSS In-Situ et Mobile) project. Authors would also thanks the farmer, Mr Blanquet, for his time and the person who helped for collecting ground data.

References

Betbeder, J., Fieuzal, R., Philippets, Y., Ferro-Famil, L., and Baup, F.: Contribution of multitemporal polarimetric synthetic aperture radar data for monitoring winter wheat and rapeseed crops, J. Appl. Remote Sens. 10(2), 026020, doi: 10.1117/1.JRS.10.026020, 2016.

Bilich, A., and Larson, K. M.: Mapping the GPS multipath environment using the signal-to-noise ratio (SNR). Radio Science, 42(6), RS6003, 2017.

Boniface, K. Braun, J. J., McCreight, J.L., and Nievinski, F.G.:.Comparison of snow data assimilation system with GPS reflectometry snow depth in the western United States. Hydrological Processes 29 (10), 2425-2437, 2015

Chew, C. C., Small, E. E., Larson, K. M., and Zavorotny, V. U.: Effects of near-surface soil moisture on GPS SNR data: development of a retrieval algorithm for soil moisture. IEEE Transactions on Geoscience and Remote Sensing, 52(1), 537-543, 2014.

Chew, C., Small, E. E., and Larson, K. M.: An algorithm for soil moisture estimation using GPS-interferometric reflectometry for bare and vegetated soil. GPS Solutions, 1-13, 2015a.

Chew, C. C., Small, E. E., Larson, K. M., and Zavorotny, V. U.: Vegetation sensing using GPS-interferometric reflectometry: theoretical effects of canopy parameters on signal-to-noise ratio data. IEEE Transactions on Geoscience and Remote Sensing, 53(5), 2755-2764, 2015b.

Decharme, B., Boone, A., Delire, C., and Noilhan, J.: Local evaluation of the Interaction between Soil Biosphere Atmosphere soil multilayer diffusion scheme using four pedotransfer functions, J. Geophys. Res., 116, D20126, doi:10.1029/2011JD016002, 2011.

Dorigo, W.A., Xaver, A., Vreugdenhil, M., Gruber, A., Hegyiová, A., Sanchis-Dufau, A.D., Zamojski, D., Cordes, C, Wagner, W, and Drusch, M.: Global automated quality control of in situ soil moisture data from the International Soil Moisture Network, Vadose Zone Journal, 12, 3, doi:10.2136/vzj2012.0097, 2013.

Fieuzal, R., Baup, F., and Marais-Sicre, C.: Monitoring wheat and rapeseed by using synchronous optical and radar satellite data—From temporal signatures to crop parameters estimation. Advances in Remote Sensing, 2(2), 33222, 2013.

Foti, G., Gommenginger, C., Jales, P., Unwin, M., Shaw, A., Robertson, C., and Rosello, J.: Spaceborne GNSS reflectometry for ocean winds: First results from the UK TechDemoSat-1 mission. Geophysical Research Letters, 42(13), 5435-5441, 2015.

Gastal, F., and Lemaire, G.: N uptake and distribution in crops: an agronomical and ecophysiological perspective, J. Exp. Bot., 53, 370, 789-799, doi: 10.1093/jexbot/53.370.789, 2002.

Georgiadou, Y.,and Kleusberg, A.: On carrier signal multipath effects in relative GPS positioning. Manuscripta geodaetica, 13(3), 172-179, 1988.

Kerr, Y., Waldteufel, P., Wigneron, J., Martinuzzi, J., Font, J., and Berger, M.: Soil moisture retrieval from space: The Soil Moisture and Ocean Salinity (SMOS) mission, IEEE T. Geosci. Remote, 39, 1729–1735, 2001.

Lafont, S., Zhao, Y., Calvet, J.-C., Peylin, P., Ciais, P., Maignan, F., and Weiss, M.: Modelling LAI, surface water and carbon fluxes at high-resolution over France: comparison of ISBA-A-gs and ORCHIDEE, Biogeosciences, 9, 439–456, doi:10.5194/bg-9-439-2012, 2012.

Larson, K. M., Small, E. E., Gutmann, E. D., Bilich, A. L., Braun, J. J., and Zavorotny, V. U.: Use of GPS receivers as a soil moisture network for water cycle studies. Geophysical Research Letters, 35(24), 2008.

Larson, K. M., Braun, J. J., Small, E. E., Zavorotny, V. U., Gutmann, E. D., and Bilich, A. L.: GPS multipath and its relation to near-surface soil moisture content. IEEE Journal of Selected Topics in Applied Earth Observations and Remote Sensing, 3(1), 91-99, 2010.

Larson, K. M., and Nievinski, F. G.: GPS snow sensing: results from the EarthScope Plate Boundary Observatory. GPS solutions, 17(1), 41-52, 2013.

Larson, K. M.; Small, E. E.; Chew, C. C.; Nievinski, F. G.; Pratt, J.; McCreight, J. L.; Braun, J.; Boniface, K.; and Evans, S. G.: PBO H2O: Plate Boundary Observatory Studies of the Water Cycle, American Geophysical Union, Fall Meeting, San Francisco, 9-13 December, 2013.

Larson, K. M., and Small, E. E.: Normalized microwave reflection index: A vegetation measurement derived from GPS networks. IEEE Journal of Selected Topics in Applied Earth Observations and Remote Sensing, 7(5), 1501-1511, 2014.

Larson, K. M.: GPS interferometric reflectometry: applications to surface soil moisture, snow depth, and vegetation water content in the western United States. Wiley Interdisciplinary Reviews: Water, 3(6), 775-787, 2016.

Masson, V., Le Moigne, P., Martin, E., Faroux, S., Alias, A., Alkama, R., Belamari, S., Barbu, A., Boone, A., Bouyssel, F., Brousseau, P., Brun, E., Calvet, J.-C., Carrer, D., Decharme, B., Delire, C., Donier, S., Essaouini, K., Gibelin, A.-L., Giordani, H., Habets, F., Jidane, M., Kerdraon, G., Kourzeneva, E., Lafaysse, M., Lafont, S., Lebeaupin Brossier, C., Lemonsu, A., Mahfouf, J.-F., Marguinaud, P., Mokhtari, M., Morin, S., Pigeon, G., Salgado, R., Seity, Y., Taillefer, F., Tanguy, G., Tulet, P., Vincendon, B., Vionnet, V., and Voldoire, A.: The SURFEXv7.2 land and ocean surface platform for coupled or offline simulation of earth surface variables and fluxes, Geosci. Model Dev., 6, 929–960, doi:10.5194/gmd-6-929-2013, 2013.

Morisette, J.T., Baret, F., Privette, J.L., Myneni, R.B., Nickeson, J.E., Garrigues, S., Shabanov, N., Weiss, M., Fernandes, R., Leblanc, S., Kalacska, M., Sánchez-Azofeifa, G.A., Chubey, M., Rivard, B., Stenberg, P., Rautiainen, M., Voipio, P., Manninen, T., Pilant, A.N., Lewis, T.E., Iiames, J.S., Colombo, R., Meroni, M., Busetto, L., Cohen, W., Turner, D.P., Warner, E.D., Petersen, G.W., Seufert, G., and Cook, R.: Validation of global moderate-resolution LAI products: A

framework proposed within the CEOS land product validation subgroup. IEEE Transactions on Geoscience and Remote Sensing, 44(7), 1804–1817, 2006.

Motte E., Egido A., Roussel N., Boniface K., and Frappart F.: Applications of GNSS-R in continental hydrology. In Baghdadi N., Zribi M. (Eds.), Land Surface Remote Sensing in Continental Hydrology, Elsevier, 281-321, doi: 10.1016/B978-1-78548-104-8.50009-7, 2016.

Njoku, E.G., Wilson, W.J., Yueh, S.H., Dinardo, S.J., Li, F.K., Jackson, T.J., Lakshmi, V. and Bolten, J.: Observations of soil moisture using a passive and active low-frequency microwave airborne sensor during SGP99. IEEE Transactions on Geoscience and Remote Sensing, 40(12), 2659-2673, doi:10.1109/TGRS.2002.807008, 2002.

Roesch, A., Schmidbauer, H., and Roesch, M. A.: Package 'WaveletComp', 2014.

Roussel, N., Frappart, F., Ramillien, G., Darrozes, J., Desjardins, C., Gegout, P., Pérosanz, F., and Biancale, R.: Simulations of direct and reflected wave trajectories for ground-based GNSS-R experiments. Geoscientific Model Development, 7, 2261-2279, 2014.

Roussel, N., Frappart, F., Ramillien, G., Darrozes, J., Baup, F., Lestarquit, L., and Ha, M. C.: Detection of Soil Moisture Variations Using GPS and GLONASS SNR Data for Elevation Angles Ranging From 2° to 70°. IEEE Journal of Selected Topics in Applied Earth Observations and Remote Sensing, 1-14, 2016.

Small, E. E., Larson, K. M., and Braun, J. J.: Sensing vegetation growth with reflected GPS signals. Geophysical Research Letters, 37(12), L12401, 2010.

Small, E. E., Larson, K. M., and Smith, W. K.: Normalized microwave reflection index: validation of vegetation water content estimates from Montana grasslands. IEEE Journal of Selected Topics in Applied Earth Observations and Remote Sensing, 7(5), 1512-1521, 2014.

Small, E. E., Larson, K. M., Chew, C. C., Dong, J., and Ochsner, T. E.: Validation of GPS-IR soil moisture retrievals: Comparison of different algorithms to remove vegetation effects. IEEE Journal of Selected Topics in Applied Earth Observations and Remote Sensing, pp(1), 1-12, 2016.

Vey, S., Güntner, A., Wickert, J., Blume, T., and Ramatschi, M.: Long-term soil moisture dynamics derived from GNSS interferometric reflectometry: A case study for Sutherland, South Africa. GPS Solutions, 1-14, 2015.

Wan, W., Larson, K. M., Small, E. E., Chew, C. C., and Braun, J. J.: Using geodetic GPS receivers to measure vegetation water content. GPS Solutions, 19(2), 237-248, 2015.

Wigneron, J.P., Ferrazzoli, P., Olioso, A., Bertuzzi, P. and Chanzy, A.: A simple approach to monitor crop biomass from C-band radar data, Remote Sens. Environ., 69, 179-188, 1999.

Zavorotny, V. U., Larson, K. M., Braun, J. J., Small, E. E., Gutmann, E. D., and Bilich, A. L.: A physical model for GPS multipath caused by land reflections: Toward bare soil moisture retrievals. IEEE Journal of Selected Topics in Applied Earth Observations and Remote Sensing, 3(1), 100-110, 2010.

Zavorotny, V. U., Gleason, S., Cardellach, E., and Camps, A.: Tutorial on remote sensing using GNSS bistatic radar of opportunity. IEEE Geoscience and Remote Sensing Magazine, 2(4), 8-45, 2014.

Hydrol. Earth Syst. Sci. Discuss., doi:10.5194/hess-2017-152, 2017
Manuscript under review for journal Hydrol. Earth Syst. Sci.
Discussion started: 22 March 2017

Hydrology and Earth System Sciences
Discussions

Table 1. Soil moisture scores from 16 January to 5 March 2015.

	GPS vs. *in situ*	GPS vs. ISBA	GPS vs. *in situ*	GPS vs. ISBA	ISBA vs. *in situ*
S ($m^3m^{-3}deg^{-1}$)	0.0148		0.0033		
N	47	43	47	43	43
MAE (m^3m^{-3})	0.036	0.034	0.011	0.018	0.009
RMSE (m^3m^{-3})	0.046	0.041	0.014	0.022	0.010
SDD (m^3m^{-3})	0.036	0.037	0.009	0.012	0.006
Mean bias (m^3m^{-3})	0.029	0.019	-0.010	-0.018	0.008
R^2	0.73	0.63	0.73	0.63	0.88

Table 2. Sub-daily variability (standard deviation, in m^3m^{-3}) of VSM estimates.

	Minimum	Maximum	Average value
In situ observations	0.000	0.009	0.002
ISBA simulations	0.000	0.021	0.005
GPS retrievals with S = 0.0148 $m^3m^{-3}deg^{-1}$	0.012	0.090	0.036
GPS retrievals with S = 0.0033 $m^3m^{-3}deg^{-1}$	0.003	0.020	0.008

Table 3. Vegetation height scores from 10 March to 11 June 2015.

	GPS vs. *in situ*	Moving average (21 days) GPS vs. *in situ*	GPS vs. ISBA	Moving average (21 days) GPS vs. ISBA	ISBA vs. *in situ*
N	5	5	87	94	5
MAE (cm)	5.5	3.7	8.9	9.0	6.8
RMSE (cm)	6.2	5.0	12.4	11.6	8.6
SDD (cm)	5.5	3.8	12.5	11.6	9.6
Mean bias (cm)	3.8	3.7	-0.6	-0.8	0.4
R^2	0.98	0.99	0.89	0.91	0.95

Hydrol. Earth Syst. Sci. Discuss., doi:10.5194/hess-2017-152, 2017
Manuscript under review for journal Hydrol. Earth Syst. Sci.
Discussion started: 22 March 2017

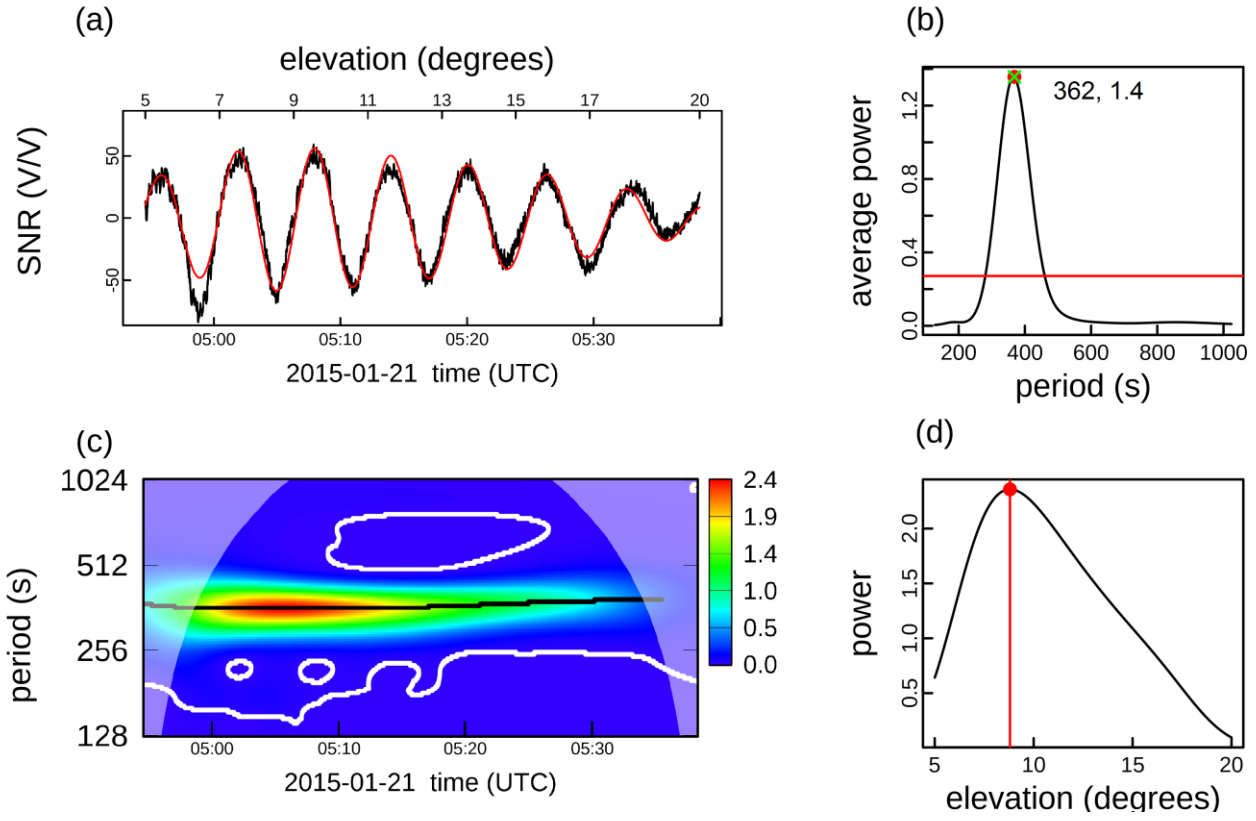

Figure 1. Example of a usable GPS01 ascending track SNR data set from 04:50 UTC to 05:38 UTC on 21 January 2015: (a) Multipath SNR data (in V V^{-1}), (b) average power spectrum and (c) power spectrum for periods from 128 to 1024 s. The red line in (a) is the reconstructed SNR data by the daughter wavelet corresponding to the peak period (362 s) indicated in (b). The power at the peak period across elevation angles (d) presents a maximum value at an elevation angle of about 9 degrees.

Hydrol. Earth Syst. Sci. Discuss., doi:10.5194/hess-2017-152, 2017
Manuscript under review for journal Hydrol. Earth Syst. Sci.
Discussion started: 22 March 2017

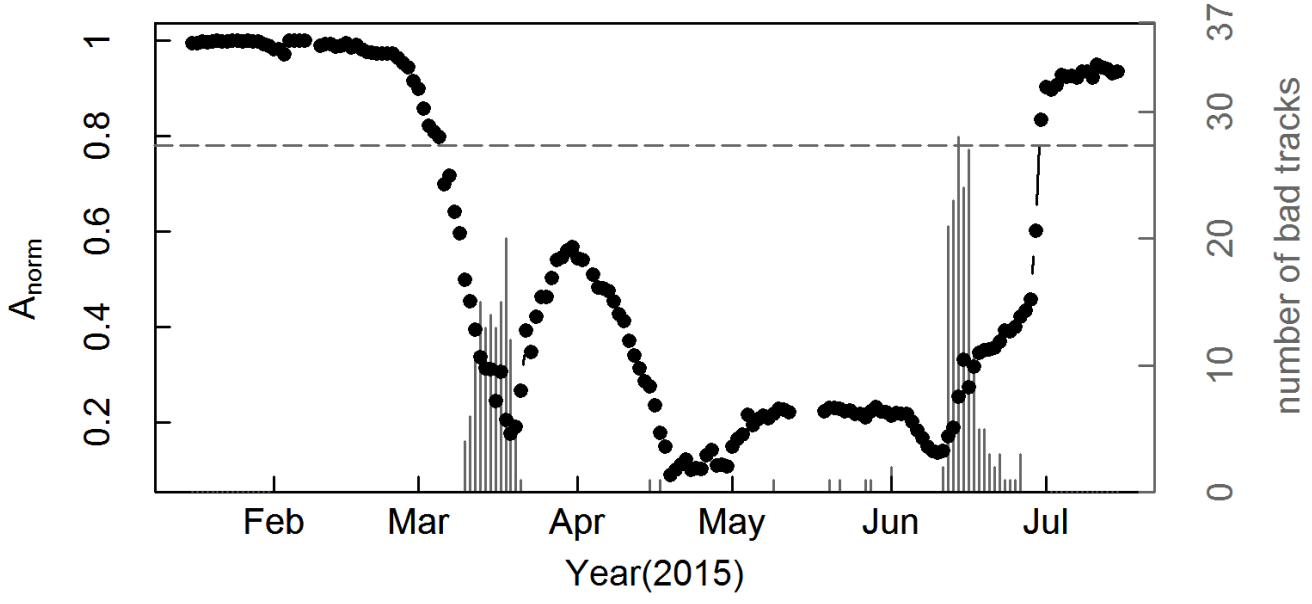

Figure 2. Normalized amplitude (A_{norm}) time series (black dots) and probability distribution (grey bars) of low quality tracks among all available satellite tracks on a daily basis from 16 January to 15 July 2015. Soil moisture can be retrieved from 16 January to 5 March 2015 because A_{norm} is larger than 0.78 (indicated by the grey dashed line).

.

Hydrol. Earth Syst. Sci. Discuss., doi:10.5194/hess-2017-152, 2017
Manuscript under review for journal Hydrol. Earth Syst. Sci.
Discussion started: 22 March 2017

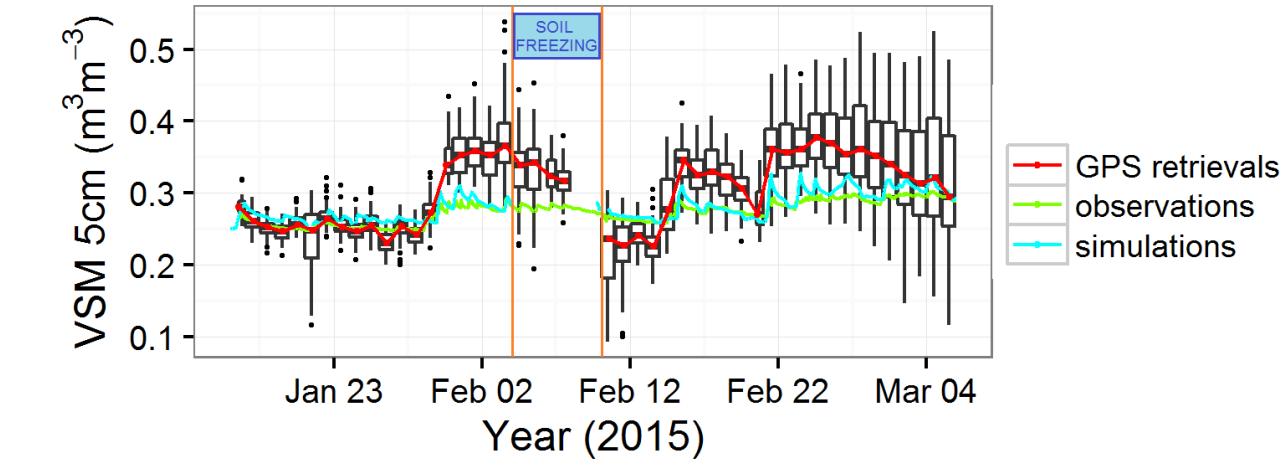

Figure 3. ***In situ*** **daily mean surface volumetric soil moisture (VSM) observations at 5 cm depth (green line), ISBA daily mean simulations (blue line), median of the daily GPS retrievals with a priori slope (S = 0.0148 $m^3m^{-3}deg^{-1}$) (red line) and their daily statistical distribution (black box plots) for all available satellite tracks from 16 January to 5 March 2015. Boxes: 25-75% percentiles; bars: maximum (minimum) values below (above) 1.5 IQR (Inter Quartile Range, corresponding to the 25-75% percentile interval); dots: data outside the 1.5 IQR interval. The ISBA simulations indicate soil freezing (i.e. the presence of ice in the top soil layer) from 4 to 9 February.**

Hydrol. Earth Syst. Sci. Discuss., doi:10.5194/hess-2017-152, 2017
Manuscript under review for journal Hydrol. Earth Syst. Sci.
Discussion started: 22 March 2017

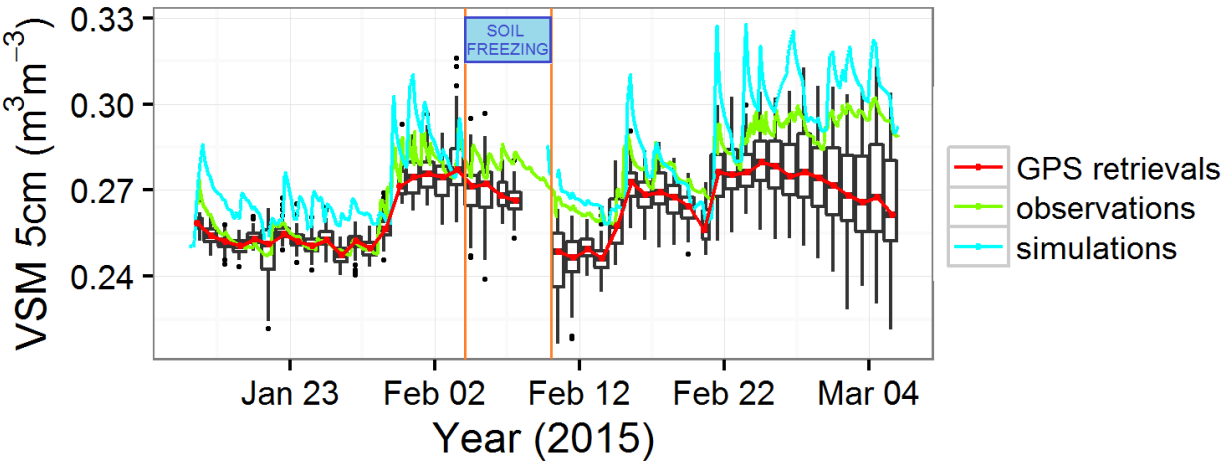

Figure 4. As in Fig. 3, except for local fitted slope (S = 0.0033 $m^3m^{-3}deg^{-1}$) (red line).

Hydrol. Earth Syst. Sci. Discuss., doi:10.5194/hess-2017-152, 2017
Manuscript under review for journal Hydrol. Earth Syst. Sci.
Discussion started: 22 March 2017

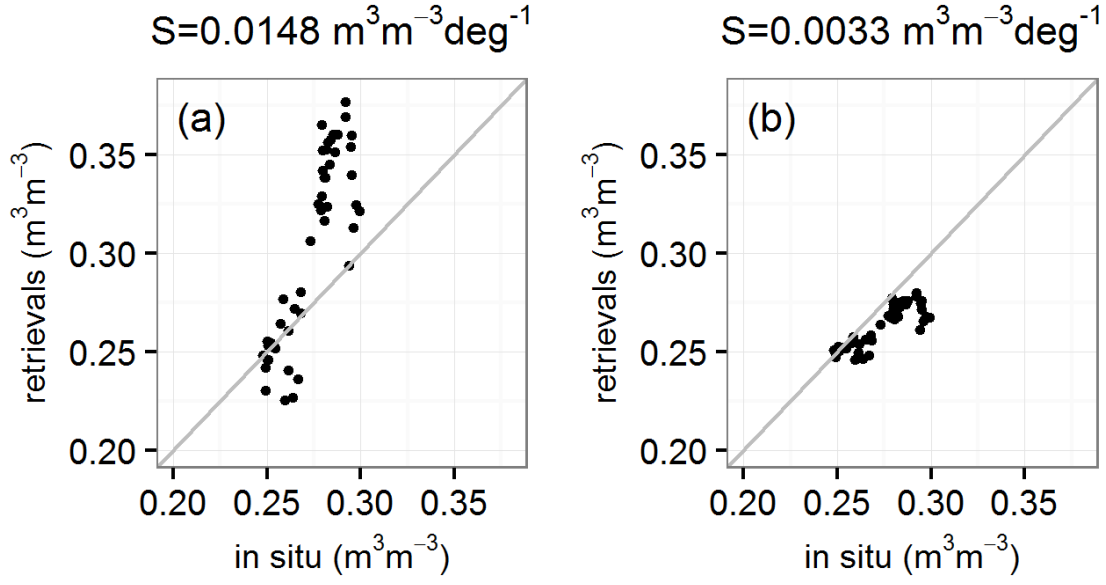

Figure 5. VSM GPS retrievals versus *in situ* VSM observations (m^3m^{-3}) from 16 January to 5 March 2015, (a) with a priori slope S=0.0148 $m^3m^{-3}deg^{-1}$, VSM=0.0148Δφ+0.252 (b) with fitted slope = 0.0033 $m^3m^{-3}deg^{-1}$, VSM=0.0033Δφ+0.252. More scores can be referred from Table 1.

Hydrol. Earth Syst. Sci. Discuss., doi:10.5194/hess-2017-152, 2017
Manuscript under review for journal Hydrol. Earth Syst. Sci.
Discussion started: 22 March 2017

Hydrology and Earth System Sciences
Discussions

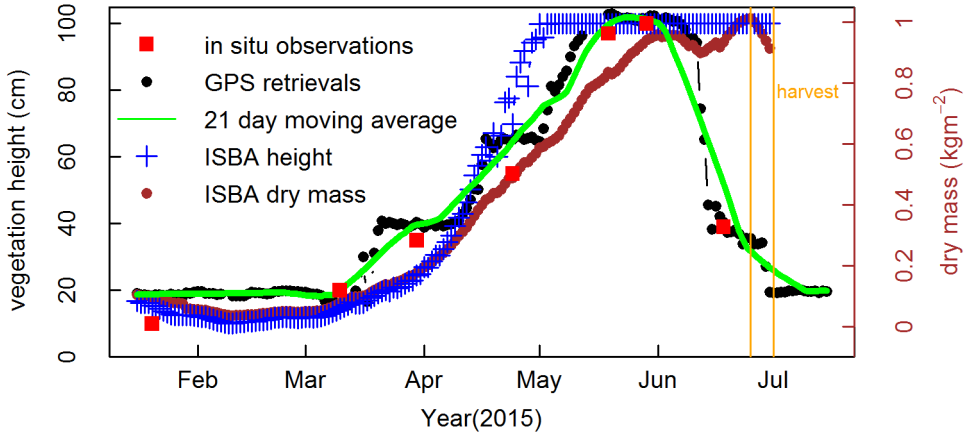

Figure 6. Wheat canopy height from 16 January to 15 July 2015 derived from GPS SNR data (black dots), from *in situ* observations (red squares), and from ISBA simulations (blue crosses). The green line represents the moving average of the GPS retrievals, computed using a centered gliding window of 21 days. Wheat above-ground biomass simulated by the ISBA model is indicated by brown dots.

Hydrol. Earth Syst. Sci. Discuss., doi:10.5194/hess-2017-152, 2017
Manuscript under review for journal Hydrol. Earth Syst. Sci.
Discussion started: 22 March 2017

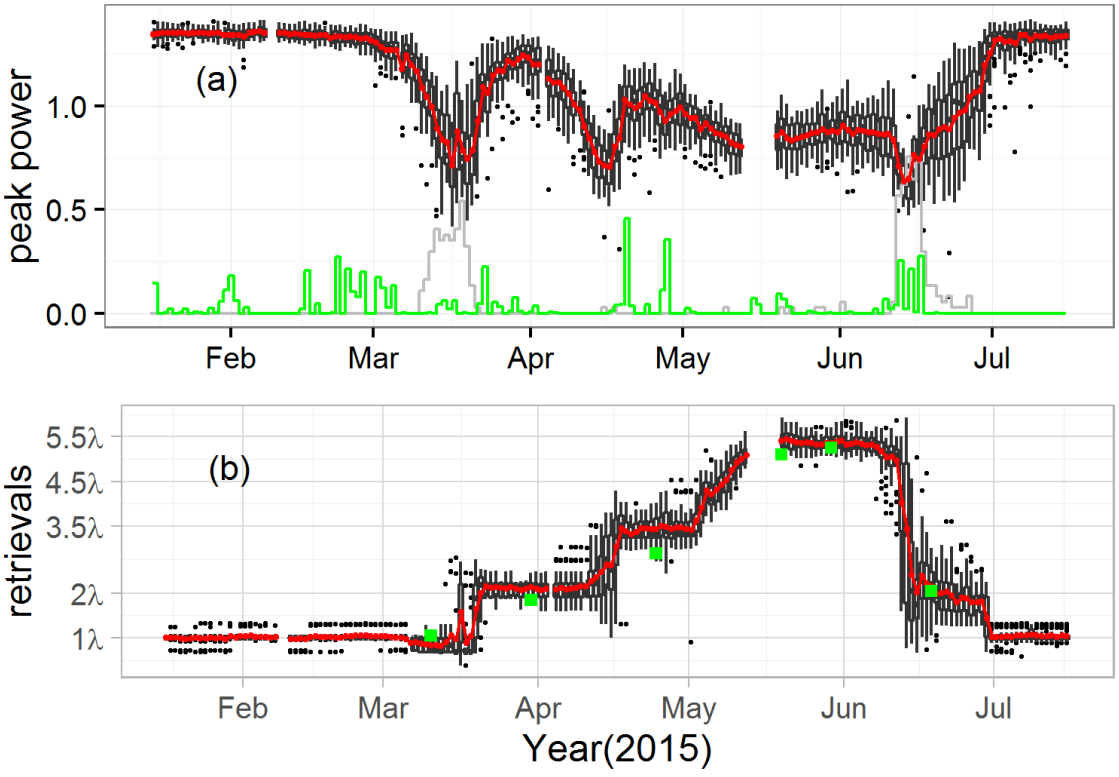

Figure 7. The box plots of (a) the peak power from a wavelet analysis and (b) the retrieved vegetation height (rescaled in λ units) for all available satellite tracks from 16 January to 15 July 2015. The mean value of the peak power and of the retrievals are shown by red lines. In (a), the grey line shows the statistical distribution of bad quality tracks (the number of the bad quality tracks can be obtained multiplying by 37), the green line represents the rainfall (daily precipitation in mm d^{-1} can be obtained multiplying by 50). In (b), the rescaled *in situ* observations are shown by green squares.